This is a previous version of the article published in Materials and Structures. 2016, 49(8): 3021-3037. doi:10.1617/s11527-015-0702-7

Improved correlation between the static and dynamic elastic modulus of different types of rocks

V. Brotons[1] *, R. Tomás[1], S. Ivorra[1], A. Grediaga[2], J. Martínez-Martínez[3,4], D. Benavente[3,4], M. Gómez-Heras[5]

(1) Department of Civil Engineering. Escuela Politécnica Superior, Universidad de Alicante, P.O. Box 99, E-03080 Alicante, Spain.

(2) Department of Information Technology and Computing. Escuela Politécnica Superior, Universidad de Alicante, P.O. Box 99, E-03080 Alicante, Spain.

(3) Applied Petrology Laboratory. Unidad Asociada CSIC-UA. Alicante. Spain.

(4) Department of Earth and Environmental Sciences. Facultad de Ciencias, Universidad de Alicante, P.O. Box 99, E-03080 Alicante, Spain.

(5) Institute of Geosciences. Unidad Asociada CSIC-UCM, Jose Antonio Novais 12, 28040 Madrid, Spain.

**Corresponding author. Tel.: +34-965-903400. E-mail address: vicente.brotons@ua.es*

Abstract

The relationship between the static and dynamic elastic modulus in rock materials has been frequently addressed in scientific literature. Overall, when it comes to the study of materials with a wide range of elastic moduli, the functions that best represent this relationship are non-linear and do not depend on a single parameter. In this study, the relationships between the static and dynamic elastic modulus of 8 different igneous, sedimentary and metamorphic rock types, all of which are widely used as construction material, were studied. To this end, the elastic modulus values of 33 samples were obtained which, together with the values obtained for 24 other samples in a previous study, allowed a new relationship between these parameters to be proposed. Firstly, linear and nonlinear classical models were used to correlate static and dynamic moduli, giving R-squared values of 0.97 and 0.99, respectively. A classical power correlation between static

modulus and P-wave velocity has also been proposed, giving an R-squared (R^2) value of 0.99 and a sum of the squared differences (SSE) of 553.93. Finally, new equations relating static and dynamic modulus values have been proposed using novel nonlinear expressions. These consider: a) bulk density (R^2=0.993 and SSE=362.66); b) bulk density and total porosity of rock (R^2=0.994 and SSE=332.16); and c) bulk density, total porosity of rock and uniaxial compressive strength (R^2=0.996 and SSE=190.27). The expressions obtained can be used to calculate the static elastic modulus using non-destructive techniques, in a broad range of rock-like materials.

Keywords: Non-destructive techniques, stone, dynamic modulus, static modulus, rock-materials, igneous, sedimentary, metamorphic.

1. INTRODUCTION

The elastic modulus is an important mechanical property of rock and stone in relation to its use as a building material. It is the parameter determining the deformability of the material under applied loads, making it an essential parameter for any structural elements (Al-Shayea 2004; Ciccotti and Mulargia 2004; Eissa and Kazi 1988). Deformability tests require samples to be extracted and loads applied to them in the laboratory. The destructive nature of this testing means that it is not suitable for use in certain situations, such as in historic buildings. Alternatively, the elastic modulus can be obtained from non-destructive testing: typically using results obtained from tests measuring the propagation velocity of ultrasonic elastic waves, also called the dynamic modulus (Ameen et al. 2009; Christaras et al. 1994; Eissa and Kazi 1988; Ide 1936; King 1983; Najibi et al. 2015). The static modulus (E_{st}), obtained from conventional laboratory mechanical procedures, is required for computing or modelling the deformations of a building under in-service loading. In cases in which it is not possible to determine the characteristics of the rock using destructive tests, the use of non-destructive techniques using mobile devices constitutes a suitable alternative (Christaras et al. 1994).

The dynamically determined elastic modulus (E_{dyn}) is generally higher than the statically determined modulus, and the values diverge greatly in rocks with a low modulus of elasticity (Ide 1936). Several studies (Al-Shayea 2004; Ide 1936; Kolesnikov 2009; Vanheerden 1987) explain these differences by considering the nonlinear elastic response at the different strain ranges (ε)

involved in the different techniques. The difference between the static and the dynamic modulus is also explained considering the effect of porosity, size and spatial orientation of cracks or bedding planes on both different measurement techniques (Al-Shayea 2004; Ameen et al. 2009; Eissa and Kazi 1988; Ide 1936; King 1983; Najibi et al. 2015; Vanheerden 1987). The static method, which is necessary for quantifying the rock's deformability, is more sensitive to the presence of discontinuities in the rock. The study of a high strength limestone (i.e. 70 MPa) (Al-Shayea 2004) showed that the ratio between moduli:

$$\mathrm{k} = \mathrm{E_{dyn}}/\mathrm{E_{st}} \quad (1)$$

is close to one when the static modulus is measured at very low loading levels (~10% of uniaxial compressive strength). The dynamic modulus ($\mathrm{E_{dyn}}$), is usually calculated from equation (2):

$$E_{dyn} = \rho_{bulk} {V_s}^2 \frac{3{V_p}^2 - 4{V_s}^2}{{V_p}^2 - {V_s}^2} \quad (2)$$

where $\mathrm{E_{dyn}}$ is the dynamic modulus of elasticity, V_p is the velocity of compression (P) waves, V_s is the shear (S) wave velocity and ρ_{bulk} is the bulk density of the material.

The relationships between the static and dynamic moduli for different types of rocks and ranges of values proposed by various authors (Brotons et al. 2014; Christaras et al. 1994; Eissa and Kazi 1988; Horsrud 2001; King 1983; Lacy 1997; Martinez-Martinez et al. 2012; Najibi et al. 2015; Nur and Wang 1999; Vanheerden 1987) are summarized in Table 1. Note that Eissa and Kazi (1988) performed a statistical analysis using 76 observations from three different sources of information, for which bulk density was known, defining twelve different variables, including E_{st}, E_{dyn} , ρ_{bulk} and other nine combinations thereof. Each variable was correlated with the remaining variables, covering all the possible combinations and concluding that as expected, the value of the static modulus of elasticity cannot be correlated using one single relationship valid for all different types of rock. This is due to the enormous variation in properties such as the rock's matrix, mineralogical composition and porosity, including the type of porosity (pore size distribution). Many of the proposed correlations are valid only for a certain rock type or range of elastic moduli. However, if a certain degree of imprecision is accepted, general correlations covering almost all types of rock may be proposed. In this study, various correlations of this type are proposed, having been

obtained from rocks whose dynamic modulus varied between 5 and 80 GPa, and including rocks of igneous, sedimentary and metamorphic origin.

Eq.	Reference	Relationship	R^2	E_{dyn} (GPa)	Rock type
(3)	(King 1983)	$E_{\mathrm{st}} = 1.26\ E_{\mathrm{dyn}} - 29.5$	0.82	40-120	Igneous-metamorphic
(4)	(Vanheerden 1987)	$E_{\mathrm{st}} = a\ {E_{\mathrm{dyn}}}^{b}$ $a\ [0.097 - 0.152]$ $b\ [1.485 - 1.388]$	-	20-135	Sandstone-granite
(5)	(Eissa and Kazi 1988)	$E_{\mathrm{st}} = 0.74E_{dyn} - 0.82$	0.70	5-130	All types
(6)	(Eissa and Kazi 1988)	$\log_{10}E_{\mathrm{st}} = 0.77\ \log_{10}(\rho_{\mathrm{bulk}}E_{\mathrm{dyn}}) + 0.02$	0.92	5-130	All types
(7)	(Christaras et al. 1994)	$E_{\mathrm{st}} = 1.05\ E_{dyn} - 3.16$	0.99	25-110	All types
(8)	(Lacy 1997)	$E_{\mathrm{st}} = 0.018\ {E_{dyn}}^{2} + 0.422\ E_{dyn}$	-	-	Sedimentary
(9)	(Nur and Wang 1999)	$E_{\mathrm{st}} = 1.153\ E_{dyn} - 15.2$	-	-	$E_{\mathrm{st}} > 15\ GPa$
(10)	(Horsrud 2001)	$E_{\mathrm{st}} = 0.076\ {V_p}^{3.23}$	-	-	Shale
(11)	(Martinez-Martinez et al. 2012)	$E_{\mathrm{st}} = \frac{E_{\mathrm{dyn}}}{3.8{\alpha_s}^{-0.68}}$	-	5-50	Limestone-marble
(12)	(Brotons et al. 2014)	$E_{\mathrm{st}} = 0.867E_{dyn} - 2.085$	0.96	5-30	Calcarenite
(13)	(Brotons et al. 2014)	$\log_{10}E_{\mathrm{st}} = 1.28\ \log_{10}(\rho_{\mathrm{bulk}}E_{\mathrm{dyn}}) - 4.71$	0.97	5-30	Calcarenite
(14)	(Najibi et al. 2015)	$E_{\mathrm{st}} = 0.014\ {E_{dyn}}^{1.96}$	0.87	13-74	Limestone
(15)	(Najibi et al. 2015)	$E_{\mathrm{st}} = 0.169\ {V_p}^{3.324}$	0.90	13-74	Limestone

Table 1. *Relationship between static (E_{st}) and dynamic (E_{dyn}) modulus proposed by different authors.*

The correlations shown in Table 1 may be grouped according to the independent variables used to predict the static modulus. This is shown in Table 2. It may be observed that, of the 13

correlations shown, 8 use the dynamic modulus as the only independent variable (types I-II-III). Of these, 5 are linear regression based (type I), 2 are exponential regression based (type III) and 1 quadratic regression based (type II). Of the remaining, 2 use both the dynamic modulus and apparent density as independent variables, using a separate exponential regression for both variables (type IV). 1 uses the dynamic modulus and spatial attenuation as variables (type VI), and finally, 2 use the P wave velocity as the independent variable in an exponential regression. This last type of equation has the advantage that the parameter required (V_p) is easily obtained, which consequently simplifies the testing necessary for obtaining the static elastic modulus - a dependent variable in all cases.

Eq. type	Relationship	Eqs.	Vars.	Fig.
I	$E_{\mathrm{st}} = a\,E_{\mathrm{dyn}} + b$	(3) (5) (7) (9) (12)	E_{dyn}	1
II	$E_{\mathrm{st}} = a\,{E_{dyn}}^{2} + b\,E_{dyn}$	(8)		
III	$E_{\mathrm{st}} = a\,{E_{dyn}}^{b}$	(4) (14)		
IV	$\log_{10}E_{\mathrm{st}} = a\log_{10}(\rho_{\mathrm{bulk}}E_{\mathrm{dyn}}) + b$	(6) (13)	ρ_{bulk} ; E_{dyn}	
V	$E_{\mathrm{st}} = a\,{V_p}^{b}$	(10) (15)	V_p	9
VI	$E_{\mathrm{st}} = \frac{E_{\mathrm{dyn}}}{3.8\,{\alpha_s}^{-0.68}}$	(11)	α_s; E_{dyn}	-

Table 2. *Correlation types. E_{st}: static modulus; E_{dyn}: dynamic modulus; ρ_{bulk}: bulk density; V_p: P-wave velocity; α_s: spatial attenuation.*

Figure 1 shows the plot of the equation types I-II-III-IV included in Table 1 for their respective ranges of validity. The relationship proposed by Martinez-Martinez et al. (2012) is not included in the plot because a function relating spatial attenuation with dynamic modulus must be assumed to allow it to be plotted. Note that in the Van Heerden's (1987) relationship, the four curves that are shown in Figure 1 correspond to four different sets of *a* and *b* values obtained for each stress level applied to the tested rock (the stresses considered were 10, 20, 30 and 40 MPa).

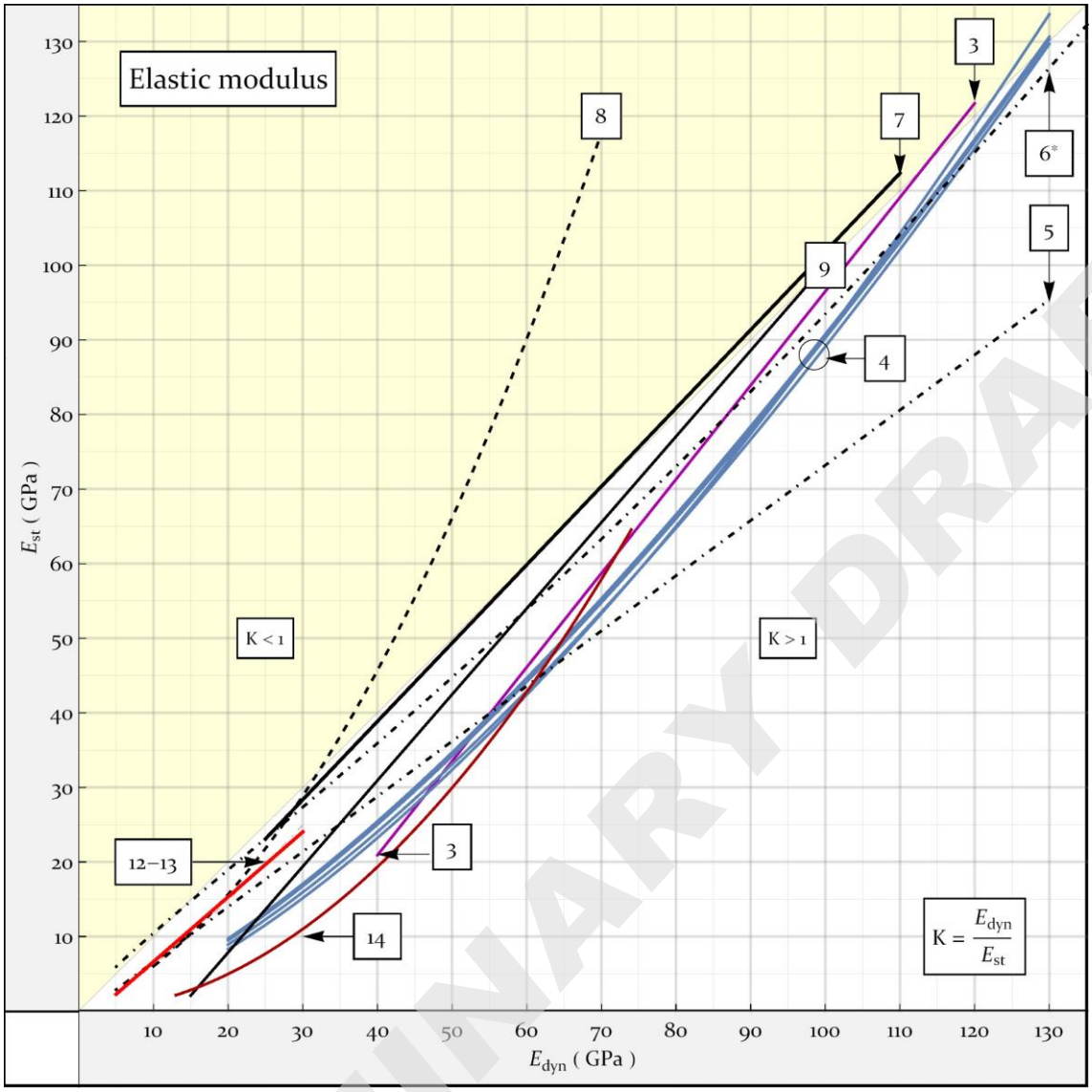

Fig. 1- Plot of the relationship between static and dynamic modulus of elasticity shown in Table 1 (Eq. types I-II-III-IV). Note that the relationships have been only represented for their range of validity. E_{st}: static modulus. E_{dyn}: dynamic modulus. The equations of the represented curves are listed in Table 1

The dimensionless coefficient k (ratio between dynamic and static modulus) (Eq. 1) has been used in their works by several authors (Martinez-Martinez et al. 2012). In Fig. 1 the line of slope 1 from the origin, represents the points where k = 1, so that the values of k>1 are located to the right of that line. For a given value of static modulus, leftmost points mean lower k values.

Consequently, the evolution of the k parameter with the module (for each curve() can be seen in Fig. 1, where, to low modulus values, in the lower left part of Fig. 1, the curves are located to the right of said diagonal line, indicating k> 1 values, and for high modulus values, in the upper right of Fig. 1, all curves (except Eq. 5 and Eq. 8) are located near the diagonal (i.e. k values that converge to unity and therefore decrease with respect to the first ones).

The general trend (except Eq. 5) shows that k decreases when dynamic modulus increases, for both linear and non-linear regressions. Therefore, it can be stated that for rocks with a high modulus of elasticity the value of k is closer to one (except Eqs. 5 and 8).

The main aim of this paper is to propose a new improved correlation for obtaining the static modulus of elasticity of a variety of rocks of different origin (widely used as structural or ornamental building materials) from non-destructive ultrasonic testing, covering a wider range of elastic modulus values (i.e. from 10 to 80 GPa).

2. MATERIALS AND SAMPLE PREPARATION

Eight different types of rock of different origin (i.e. igneous, sedimentary and metamorphic), were selected for this study. Figure 2 shows the mesoscopic appearance of the rocks used in this study. A brief petrologic description is included below.

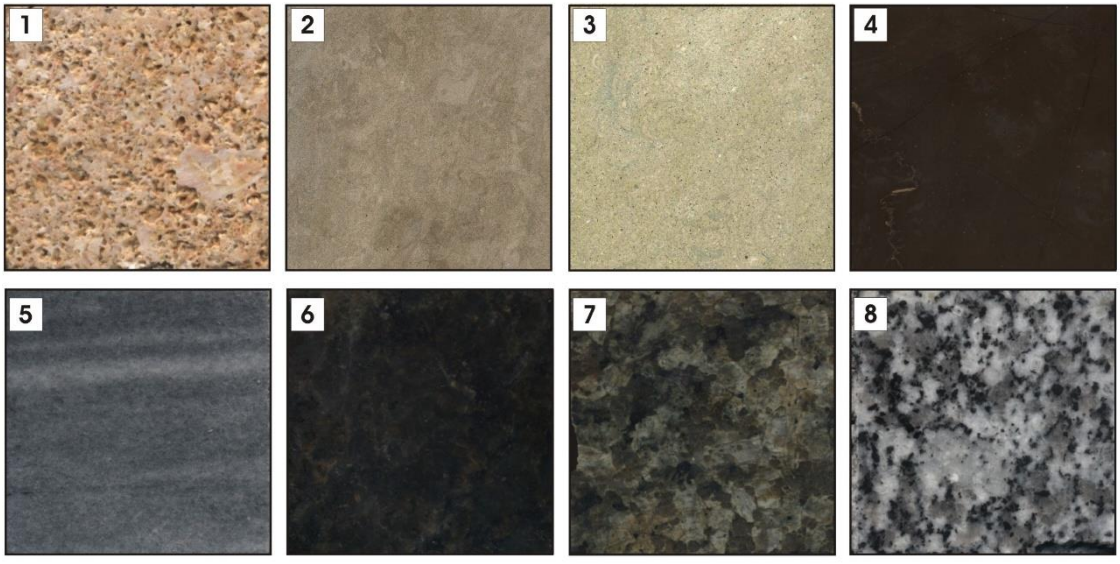

Figure 2: Rocks used in study: 1) Biocalcirudite-Golden Shell (Bcr-GS); 2) Biocalcarenite-Bateig (Bc-Ba); 3) Biocalcarenite-San Julián (Bc-SJ); 4) Micritic limestone-Gris Pulpis (ML-GP); 5)

Marble-Gris Macael (Ma-GM); 6) Monzodiorite-Verde Labrador (Mo-VL); 7) Granite-Alkaline (Gr-Fs); 8) Granite-Zarzalejo (Gr-Za). The edge length of the each image is 5 cm.

Micritic limestone - *Gris Pulpis* (ML-GP): homogeneous micritic limestone (Mudstone, according to Dunham's (1962) classification). It has a very low porosity, mainly intercrystalline. The predominant mineral is calcite, with low dolomite content. In addition, small quantities of detritic quartz, as well as pyrite (small crystals and aggregates), microcrystalline silica and fluorite were observed with optical and scanning electronic microscopy (Benavente et al. 2005).

Marble-*Gris Macael* (Ma-GM): a calcitic marble characterized by a strongly marked metamorphic banding. This lithotype is characterized by the largest crystal size (400-650 micron). The main components are: calcite and dolomite. Other components are quartz, plagioclase (albite) and muscovite. It is a low porous rocks and presents intercrystalline fissures.

Biocalcarenite-*Bateig* (Bc-Ba): a highly homogenous porous biocalcarenite, classified as packstone (according to Dunham, (1962)). The grain size is generally smaller than 1 mm. The predominant mineral is calcite, with moderate amounts of quartz and glauconitic clay. Dolomite and iron oxide can occasionally be detected. Interparticle porosity is observed in this porous rock.

Biocalcirudite. *Golden Shell* (Bcr-GS): a porous carbonate rock (grainstone after Dunham, (1962)) with abundant allochemicals consisting of grains in the 2-3 mm size range and a well-connected porous system where pores can reach up to several millimeters in size. The orthochemical fraction mainly corresponds to sparite. The predominant mineral is calcite. Both interparticle and intraparticle porosity are variable.

Granite-*Zarzalejo* (Gr-Za): a monzogranite with medium-coarse crystal size. This is an inequigranular, holocrystalline igneous rock dominated by plagioclase (30%), alkali feldspar (35%), quartz (20%), biotite (10%) and hornblende with accessory chlorite, titanite and zircon. This rock presents low open porosity and most usually is intercrystalline fissures.

Monzodiorite-*Verde Labrador* (Mo-VL): a coarse-grained rock whose crystal size lies between 2-4 mm and the most important kind of porosity is intercrysalline fissures. The main mineralogy is quartz, feldspar and plagioclase with accessory mica, pyroxene, amphibole and olivine.

Granite - Alkali (Gr-Fs): an igneous rock containing phenocrysts in a fine-grained groundmass. Phenocrysts of white feldspar up to 10 mm long are surrounded by a coarse groundmass of quartz, biotite and white feldspar. Its granitic composition is essentially quartz and potassium feldspar and its porosity is mainly intercrystalline fissures.

Biocalcarenite - *San Julián* (Bc-SJ): a very porous biocalcarenite. In terms of texture, the rock shows abundant allochemicals, generally smaller than 2 mm in size, although bands of various grain sizes have been found. The rock presents a wide variety of fossil bryozoans, foraminifera, red algae, echinoderms fragments and porosity is interparticle. The ortochemical fraction mainly corresponds to sparite. The main components are: calcite (70 %), iron-rich dolomite (25 %), quartz (5 %) and traces of clay minerals (illite) (Brotons et al. 2013).

Figure 3 shows the pore structure properties of the most representative rocks using a polarizing optical microscope (Zeiss Axioskop) and mercury intrusion porosimetry (Autopore IV 9500 Micromeritics).

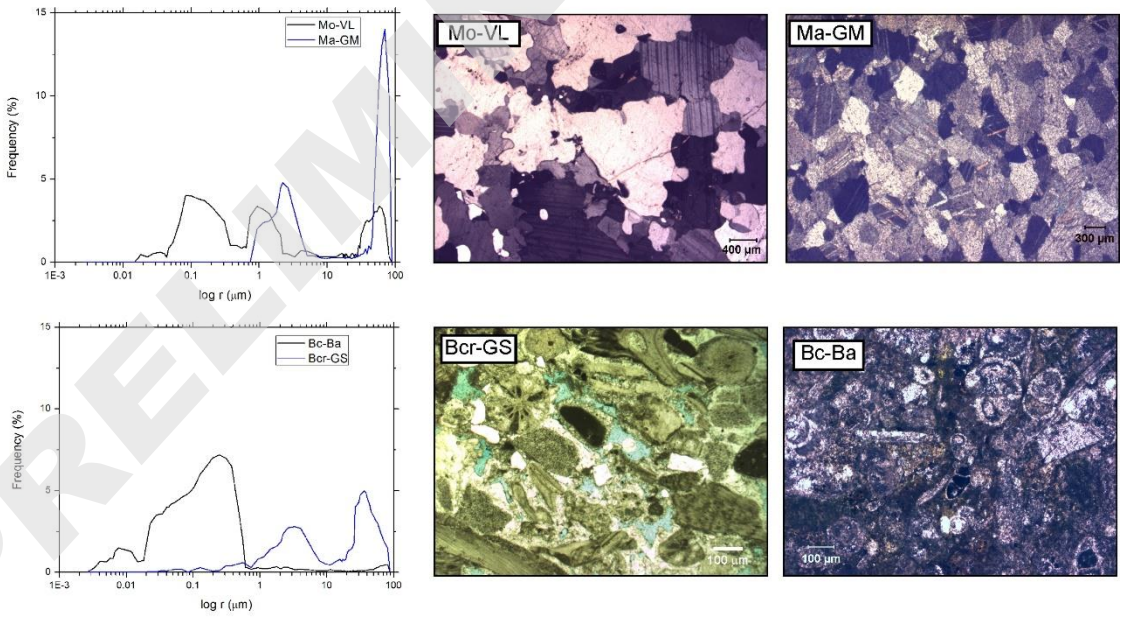

Fig. 3. Microestructure propierties of the most representative rocks. Pore size distribution of the mercury intrusion porosimetry and optical microphotographs of crystalline rocks (granite Mo-VL and marble Ma-GM) and porous rocks (biocalcarenite Bc-Ba and biocalcirrudite Bcr-GS). Mo-VL and Ma-GM microphotographs were taken under crossed-nicols, whereas Bc-Ba and Bcr-GS under parallel-nicols.

3. METHODOLOGY

For this study, 33 cylindrical samples 28 mm in diameter and 70-75 mm long were obtained (the number of cores for each rock can be found in Table 3). The choice of a minimum 2.5 slenderness ratio was made to ensure that the samples conformed to the relevant test standards (ISRM 1979).

Petro-physical property testing, including bulk and solid density, open and total porosity, P and V ultrasonic velocities, uniaxial compressive strength and both static and dynamic elastic modulus, was performed on the same core samples.

3.1. Porosity

Total porosity (n) that corresponds to the non-interconnected voids trapped in the solid phase, is calculated as the ratio of the volume of pore space to the bulk material volume, and was calculated using the relationship between bulk and solid densities. Bulk density was determined through direct measurement of the dry weight and dimensions of samples. Solid or grain density of a material is defined as the ratio of its mass to its solid volume and was obtained via the pycnometer method according to UNE-EN 1936 (AENOR 2007). Open porosity, n_0, (defined as the fraction of volume that is occupied by the fluid in the interconnected porous network) was obtained using the vacuum water saturation test UNE-EN 1936 (AENOR 2007).

Total porosity (PT) includes open porosity and close porosity. Open porosity is the volume of pores accessible to any given molecule, and close porosity is the volume of isolated pores dispersed over the medium. It is important to mention here that connected porosity is the volume of pores accessible to a given molecule and depends on the used technique.

3.2. Ultrasonic testing

Ultrasonic waves were measured using signal emitting-receiving equipment (Proceq Pundit Lab+) coupled to a computer, which acquires waveforms allowing them to be displayed, manipulated and stored. Two different kinds of transducers were used: a P-polarized transducer couple (Proceq P/N325-54 KHz) and an S-polarized transducer couple (Olympus Panametrics NDT-250 KHz). The first couple was used in order to acquire the ultrasonic P-wave waveform (longitudinal) and thereafter to study and quantify the signal in the time-domain. The second ultrasonic transducer couple was employed for the same purpose, exclusively to measure the S-wave propagation velocity. A visco-elastic couplant was used to achieve good coupling between the transducer and the sample. Two different ultrasonic parameters were computed from each registered waveform: ultrasonic P-wave velocity (V_p) and ultrasonic S-wave velocity (V_s). P-wave velocity (V_p) is the most widely-used ultrasonic parameter, and was determined from the ratio of the length of the specimen to the transit time of the pulse. The ultrasonic parameters, ultrasonic P-wave velocity (V_p) and ultrasonic S-wave velocity (V_s), were used to calculate the dynamic elastic modulus of the specimens (E_{dyn}), according to Equation (2). The UNE-EN 14579 (AENOR 2005) standard was used to determine the P wave velocity. The elastic wave velocities were measured at room pressure, and the samples were dried before testing.

3.3. Uniaxial compressive strength and deformability test

For the mechanical tests, a servo-controlled press machine with a 200 kN capacity was used for both the determination of the uniaxial compressive strength and the elastic modulus (E_{st}). The test was performed using the test method proposed by the (ISRM 1979) for the secant modulus of elasticity. Axial strain values were obtained for each loading cycle up to a maximum value equal to 40% of the sample's ultimate load. The specimen's strains were measured by means of the device shown in Figure 4. This device has two metal rings of 35 mm inside diameter attached and placed in parallel along the sample's axis, and two diametrically opposed inductive displacement sensors for measuring the relative distance between the two rings (i.e. the axial strain of the sample) during the application of the axial load. An HBM Spider 8-600 Hz data acquisition system

was used, together with “Catman-easy” software used for storing data for post-processing. According to the test method used, the stress rate was of 0.6 MPa/s, and the samples were dried before testing.

263

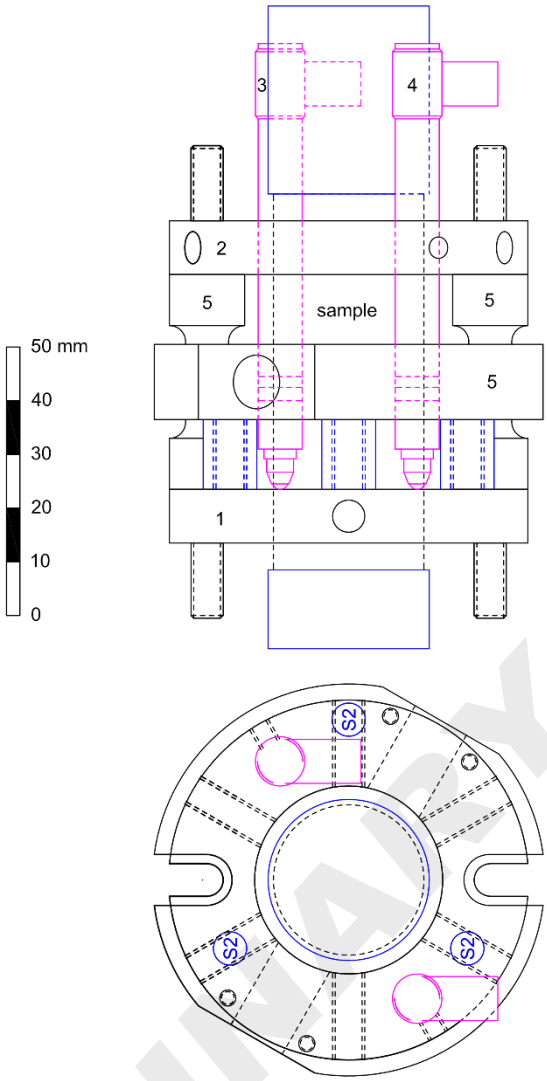

264 ***Fig. 4.*** *Device for axial strain measurements.1, 2: Rings attached to the samples; 3, 4: inductive*

265 *displacement sensors; 5: auxiliary mounting parts.*

266

267

4. RESULTS

The physical characteristics of the eight rock types included in this study are shown in Table 3. The values shown are the averages obtained for each rock type. It may be observed that the sedimentary rocks with bioclasts (Bc-Ba, Bcr-GS, Bc-SJ) showed high porosity values, which is reflected in the relatively lower apparent density. The igneous rocks (Gr-Za, Mo-VL, Gr-Pl) showed a low porosity. The lowest porosity was found in the marble (Ma-GM), which is a metamorphic rock. The micritic limestone (ML-GP) also showed a low porosity, similar to the igneous rocks.

	Rock type	Samples	Bulk Density		Open Porosity		Total Porosity	
		-	ρ_{bulk}		n_0		n	
		ud.	g/cm³		%		%	
			μ	σ	μ	σ	μ	σ
Bc-SJ	Sedimentary	5	2,096	*± 0,017*	19,597	*± 0,226*	22,499	*± 0,630*
Bc-Ba	Sedimentary	5	2,216	*± 0,014*	13,507	*± 0,768*	16,972	*± 0,506*
Bcr-GS	Sedimentary	3	2,159	*± 0,050*	11,936	*± 0,376*	17,023	*± 1,929*
Ma-GM	Metamorphic	4	2,703	*± 0,002*	0,419	*± 0,053*	0,589	*± 0,083*
Mo-VL	Igneous	4	2,634	*± 0,003*	0,916	*± 0,058*	1,306	*± 0,110*
Gr-Za	Igneous	5	2,667	*± 0,002*	0,845	*± 0,044*	1,114	*± 0,090*
Gr-Fs	Igneous	4	2,619	*± 0,009*	0,846	*± 0,068*	1,609	*± 0,321*
ML-GP	Sedimentary	3	2,674	*± 0,003*	0,847	*± 0,082*	1,065	*± 0,096*

Table 3. *Summary of physical properties of the rock samples in this study: Bc-SJ: Biocalcarenite-San Julián; Bc-Ba: Biocalcarenite-Bateig; Bcr-GS: Biocalcirudite-Golden Shell; Ma-GM: Marble-Gris Macael; Mo-VL: Monzodiorite-Verde Labrador; Gr-Za: Granite-Zarzalejo; Gr-Fs: Granite-Alkaline; ML-GP: Micritic limestone-Gris Pulpis; μ: average value; σ: Standard Deviation.*

The porosity of all of the rocks in the study was principally open, although closed porosity was significant in some rocks (especially those of igneous origin). In general, the closed porosity in the sedimentary rocks varied between 2.90 percentage points (Bc-SJ) and 5.09 percentage points (Bcr-GS). In the metamorphic rock (Ma-GM), the closed porosity was 0.17 percentage points, while in the igneous rocks the closed porosity varied between 0.27 percentage points (Gr-Za) and 0.76 percentage points (Gr-Fs).

	Rock type	Samples	Dynamic modulus		Static modulus		U. Compressive Strength	
		-	E_{dyn}		E_{st}		UCS	
		ud.	GPa		GPa		MPa	
			μ	σ	μ	σ	μ	σ
Bc-SJ	Sedimentary	5	28,52	*± 0,66*	23,84	*± 1,05*	23,61	*± 3,12*
Bc-Ba	Sedimentary	5	29,47	*± 0,71*	22,10	*± 1,13*	44,57	*± 0,97*
Bcr-GS	Sedimentary	3	33,98	*± 2,29*	30,93	*± 2,49*	23,48	*± 2,22*
Ma-GM	Metamorphic	4	46,19	*± 1,80*	39,58	*± 5,33*	31,33	*± 6,81*
Mo-VL	Igneous	4	46,40	*± 3,98*	39,80	*± 4,31*	59,86	*± 6,39*
Gr-Za	Igneous	5	52,12	*± 3,49*	41,72	*± 1,59*	56,46	*± 6,35*
Gr-Fs	Igneous	4	56,11	*± 4,15*	48,00	*± 3,70*	84,98	*± 11,80*
ML-GP	Sedimentary	3	79,14	*± 1,33*	75,83	*± 2,48*	98,81	*± 10,84*

Table 4. *Mechanical properties of the rock samples in the study: Bc-SJ: Biocalcarenite-San Julián; Bc-Ba: Biocalcarenite-Bateig; Bcr-GS: Biocalcirudite-Golden Shell; Ma-GM: Marble-Gris Macael; Mo-VL: Monzodiorite-Verde Labrador; Gr-Za: Granite-Zarzalejo; Gr-Fs: Granite-Alkaline; ML-GP: Micritic limestone-Gris Pulpis; μ: average value; σ: Standard Deviation.*

Table 4 shows the mechanical properties obtained for the rocks in the study. Regarding the elastic moduli, in all cases the dynamic moduli were greater than the static moduli.

The highest absolute elastic modulus value was observed in the micritic limestone (ML-GP). The igneous rocks (Gr-Za, Mo-VL, Gr-Fs) and marble (Ma-GM) showed intermediate values, and the sedimentary rocks with bioclasts (Bc-Ba, Bcr-GS, Bc-SJ) showed the lowest values.

The greatest resistance to uniaxial compression was observed in the rock with the greatest elastic modulus (ML-GP). The rocks with bioclasts (Bc-Ba, Bcr-GS, Bc-SJ) showed the lowest compressive strength values, with the exception of Bc-Ba, which has an exceptionally high compressive strength for this type of rock. The igneous rocks (Gr-Za, Mo-VL, Gr-Fs) showed high or very high compressive strength, and the marble (Ma-GM) a moderate value.

Figure 5 shows the dynamic (E_{dyn}) and static (E_{st}) elastic moduli obtained by ultrasonic wave propagation and mechanical testing respectively. In each type of rock the maximum and minimum values and the two central quartiles are shown in a box plot.

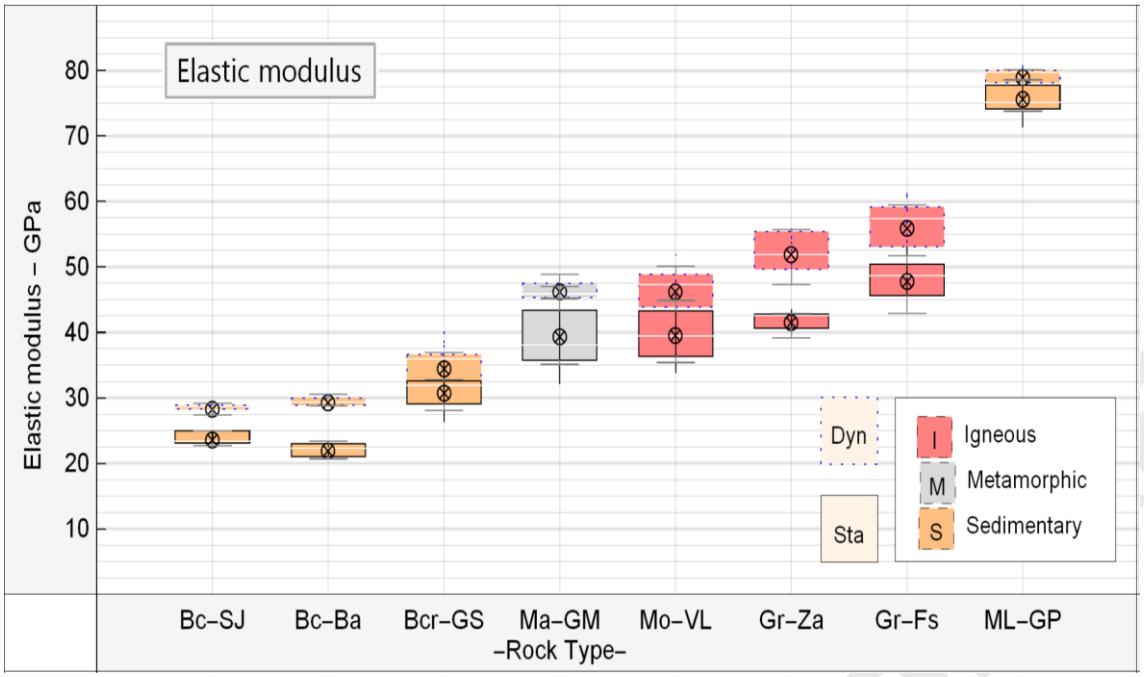

Fig. 5. *Elastic modulus of the rocks in study: Bc-SJ: Biocalcarenite-San Julián; Bc-Ba: Biocalcarenite-Bateig; Bcr-GS: Biocalcirudite-Golden Shell; Ma-GM: Marble-Gris Macael; Mo-VL: Monzodiorite-Verde Labrador; Gr-Za: Granite-Zarzalejo; Gr-Fs: Granite-Alkaline; ML-GP: Micritic limestone-Gris Pulpis.*

The bioclastic sedimentary rocks (Bc-Ba, Bcr-GS, Bc-SJ) were situated within the range of elastic moduli lower than 35 GPa, the igneous rocks (Gr-Za, Mo-VL, Gr-Fs) and marble (Ma-GM) show values in the 35-60 GPa range, and finally the micritic limestone (ML-GP) showed a static modulus of almost 80 GPa. It may be appreciated that in general the dispersion of dynamic modulus values was less than that of the static modulus values.

Figure 6 shows the uniaxial compressive strength values obtained for the samples in a box plot, as in the previous figures. The rocks with the lowest compressive strength were the sedimentary rocks with bioclasts (Bc-Ba; Bcr-GS; Bc-SJ), and additionally the marble (Ma-GM). The greatest compressive strength was observed in the micritic limestone (ML-GP). The intermediate values were observed in the igneous rocks (Gr-Za; *Mo-VL; Gr-Fs*).

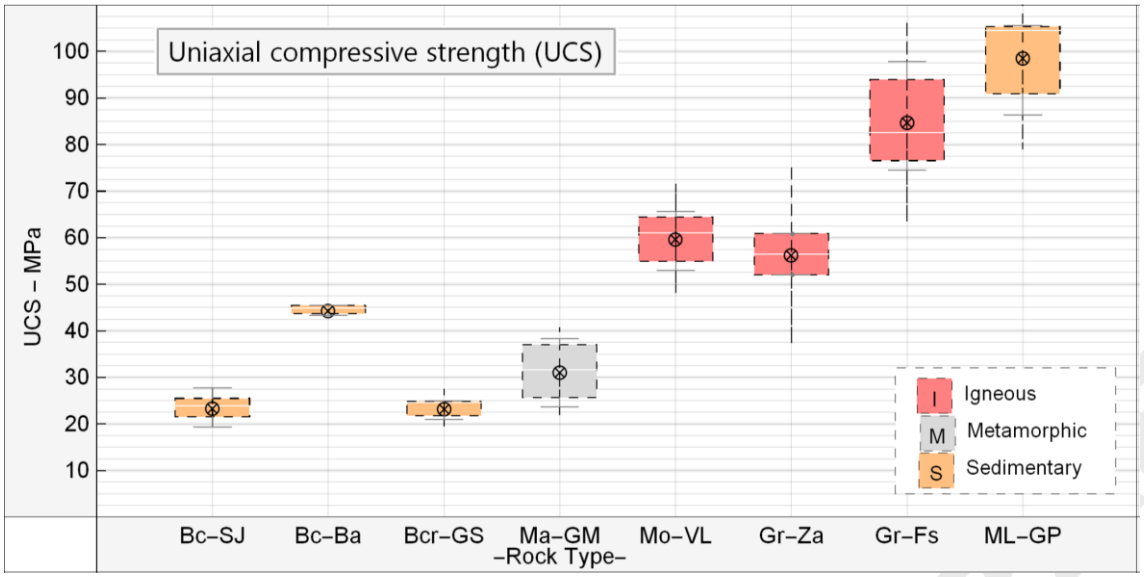

Fig. 6. *Uniaxial compressive strength (UCS) of the rocks in the study: Bc-SJ: Biocalcarenite-San Julián; Bc-Ba: Biocalcarenite-Bateig; Bcr-GS: Biocalcirudite-Golden Shell; Ma-GM: Marble-Gris Macael; Mo-VL: Monzodiorite-Verde Labrador; Gr-Za: Granite-Zarzalejo; Gr-Fs: Granite-Alkaline; ML-GP: Micritic limestone-Gris Pulpis.*

5. DISCUSSION

5.1. Discussion

The mechanical properties obtained in this study show a clear dependence on petrography. All of the rocks showed an extremely homogenous texture (free from fractures, veins, stylotites, large cavities, etc.), which suggests that the petro-physical differences between the rocks were due to: i) mineralogical differences, ii) differences in grain/crystal size, iii) differences in porosity, iv) differences in pore size.

Indeed, the differences between static and dynamic modules are explained by different authors as being due to the presence of fractures, cracks, cavities and planes of weakness and foliation (Al-Shayea 2004; Guéguen and Palciauskas 1994). In general, the more discontinuities in the rock, the lower the Young's modulus value and the higher the discrepancy between the static and dynamic values.

The petrographic parameter which most influenced the mechanical behaviour of the rocks in the study was porosity. Figure 7 shows the relationship between E_{dyn}, E_{st}, Vp and porosity. All the graphs show a similar trend. It is possible to observe two sample groups: the porous rocks group (Bc-Ba; Bcr-GS; Bc-SJ; and ML-GP) and the crystalline rocks group (Ma-GM; Mo-VL; Gr-Za; and Gr-Fs). Both the percentage of pores contained with a rock and the porosity type (pores or microcracks) have a great influence on its stiffness. The trend observed in porous rocks was that the static elastic modulus was inversely proportional to porosity. Consequentially, the micritic limestone (ML-GP), which had the lowest porosity, showed the greatest static modulus. This agrees with previous results obtained for rocks with differing porosity and porosity type (García-del-Cura et al. 2012). According to their porosity, crystalline rocks present lower values of E_{dyn}, E_{st} and Vp than those expected. This is due to the fact that their porous system is constituted by a dense microcrack net. Several authors prove that this type of porosity has a potentially great influence on the statically and dynamically measured values of Young's modulus (Heap et al., 2014).

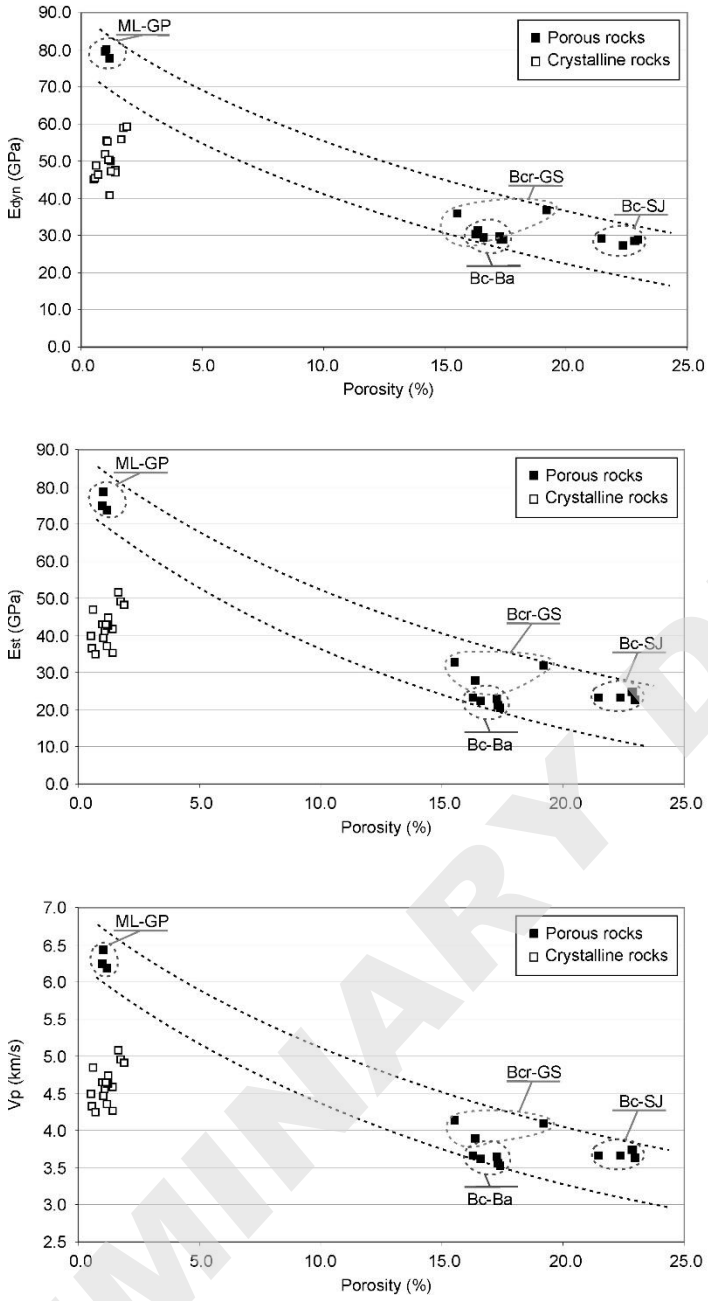

Fig. 7. *Graphs showing the relationship between porosity and the dynamic Young's modulus (E_{dyn}) (upper graph); static Young's modulus (E_{st}) (middle graph) and P-wave propagation velocity (Vp) (lower graph).*

Porosity also had the greatest influence on the ultrasonic wave propagation velocity (Fig. 7). The trend showed in this graph is the same that those described for the relationship E_{st}-porosity. Propagation velocity in porous rocks was inversely proportional to porosity, owing to the dispersion and slight delay that an ultrasonic wave experiences when passing between a solid

medium (base rock) and a fluid phase (pore) (Assefa et al. 2003; Benson et al. 2005; Martinez-Martinez et al. 2011; Vergara et al. 2001). The crystalline rocks (igneous rocks and marble) are all of them included in the same cluster in the corresponding graph of Fig. 7. This is due to the fact that these rocks show very slight differences in their porous content and they present the same type of porosity (intercrystalline). These porous are gaps between the constitutive elements of the rock (crystals) and P-wave can not be propagated through the material avoiding these gaps. Crystalline rocks act as non-continuous solid, while porous rocks with interparticle porosity act as a more continuous solid due to the presence of cements and matrix between grains. The consequence is Vp values much lower in crystalline rocks than those obtained for porous rocks with similar porous content. As the dynamic elastic modulus was obtained from the propagation velocity and density of the rock (as per Equation (2)), E_{dyn} present the same trends and the same relationship with porosity than that describes for Vp.

It was observed that mineralogy had a much lesser influence on the elastic modulus of the rocks in the study. A clear example may be seen in Figure 4. The calcitic marble (Ma-GM) and the igneous rock MO-VL are two kinds of crystalline rocks with similar porous system characteristics but their mineralogy are completely different. However, they give the same range of E_{dyn} and E_{st} values.. This has been corroborated by numerous previous studies, in which the mineralogy of rocks was shown to have little influence on their elastic behaviour, when compared to that of other factors such as porosity, the presence of fissures or crystal size (Heap and Faulkner 2008; Palchik and Hatzor 2002). Moreover, only slight differences exist between the specific P-wave velocity of the rock forming minerals of the studied rocks ($Vp_{calcite}$= 6.65 km/s; Vp_{quartz}=6.06 km/s; $Vp_{Ca\text{-}plagioclase}$ = 7.05 km/s; $Vp_{K\text{-}feldespar}$ = 5.59 km/s; according to Guéguen and Palciauskas (1994). As a consequence, no significant differences in Vp neither in E_{dyn} can be explained based on the different mineralogy between carbonate and no-carbonate rocks.

As such, porosity was practically the only petrographic parameter that influenced the elastic modulus (both static and dynamic). This simple and direct relationship between porosity and elastic modulus (E_{dyn} or E_{st}) explains the correlation between the static and dynamic modulus observed in this study.

The k-values obtained in this study according to eq. (1) vary from 1.02 to 1.42 (Figure 6). Other authors obtained values between 0.85 and 1.86 (Al-Shayea 2004; Eissa and Kazi 1988; King

1983; Vanheerden 1987). Martínez-Martínez et al. (2012) found k-values between 0.5 and 2.1 for carbonate rocks subjected to different aging conditions. These k-values tended to 1 in samples with the greatest elastic modulus values (>80 GPa). In the lowest range of elastic modulus values, the rate of increase in *k* diminished, proportional to the decrease in elastic modulus (see Fig. 8).

Figure 8 shows the dynamic and static modulus values (X and Y axis, respectively) obtained for the 33 samples tested as part of this study, as well as those of 24 samples with dynamic moduli lower than 30 GPa, tested as part of a previous study (Brotons et al. 2014). The range of *k* values in the previous study was 1.13 to 2.28.

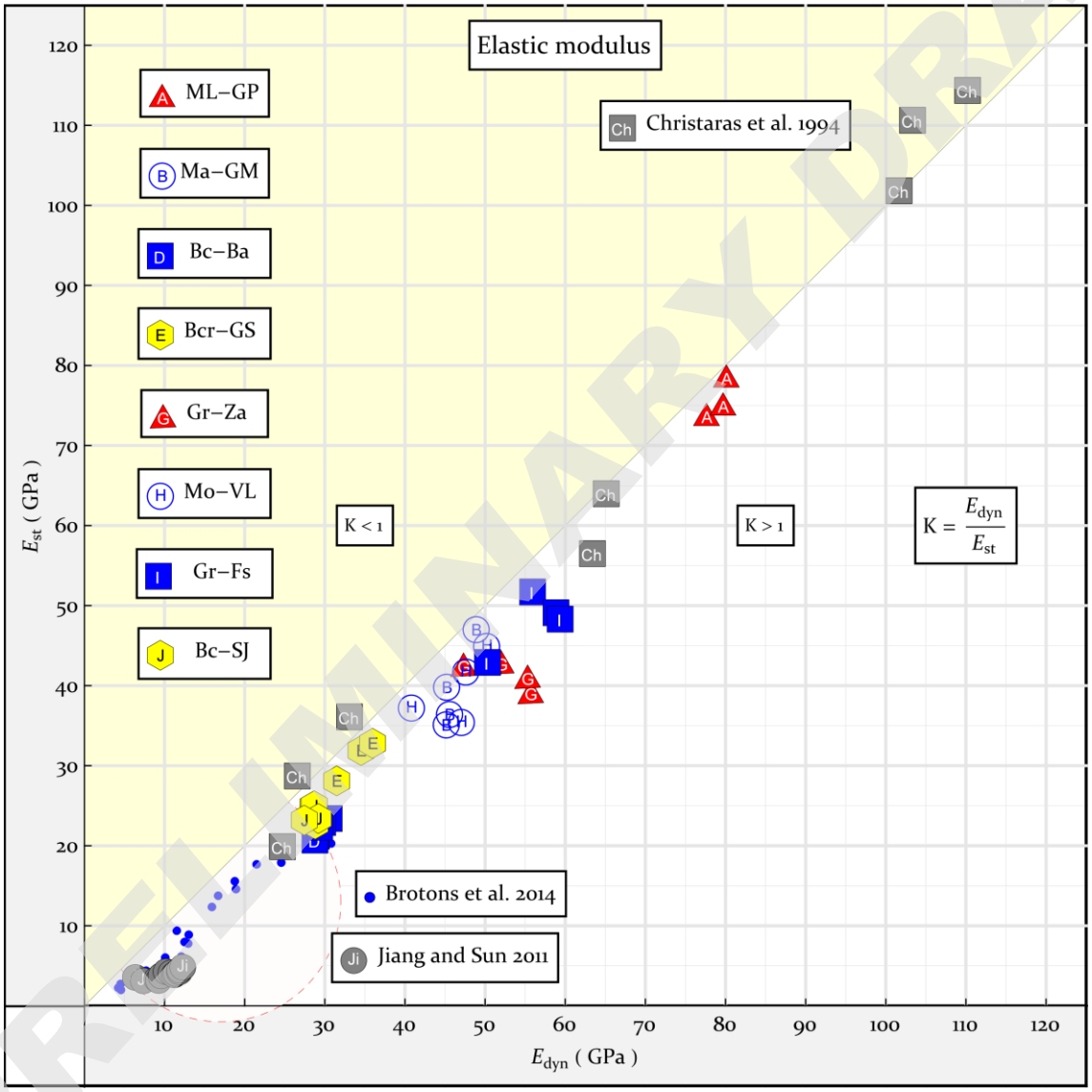

Fig. 8 - *Static and dynamic elastic modulus of samples: Blue points correspond to the samples tested in a previous study. ML-GP: Micritic limestone-Gris Pulpis; Ma-GM: Marble-Gris Macael; Bc-Ba: Biocalcarenite-Bateig; Bcr-GS: Biocalcirudite-Golden Shell; Gr-Za: Granite-Zarzalejo; Mo-*

VL: Monzodiorite-Verde Labrador; Gr-Fs: Granite-Alkaline; Bc-SJ: Biocalcarenite-San Julián; E_{st}: static modulus; E_{dyn}: dynamic modulus.

Although the values were not adjusted using the regression parameters obtained in this study, data corresponding to 12 samples tested as part of a study by Jiang and Sun (2011) has been included in Figures 8 and 9. The rock considered was a sandstone with a range of dynamic modulus values of 6-12 GPa. The range of *k* values was 1.79-2.55, and an increase in *k* in samples with a lower dynamic modulus was also observed. The authors of this study did not perform any regression analysis of their data, given the minimal variation observed. Data from a study by Christaras et al. (1994), corresponding to 8 different rock types with elastic moduli in the 25-115 GPa range is also included (shown as Ch in Figures 8 and 9), although this data was not used in the regression analysis performed as part of this study. The regression line proposed by these authors is included in Figure 1.

5.2. Fitting of data to classic models

This study builds upon the experience of previous work (Brotons et al. 2014), in order to fit the data obtained to classical models. The data obtained from the 33 samples tested as part of this study, as well as that of 24 samples tested as part of a previous study by the authors (Brotons et al. 2014), was fitted to two types of regression equations. These were:

a) Type I linear regression (see Table 2), between the static and dynamic modulus, giving R^2=0.97:

$$E_{\mathrm{st}} = 0.932\ E_{\mathrm{dyn}} - 3.421 \tag{16}$$

b) Type IV non-linear regression (see Table 2), relating the logarithm of the static modulus and the logarithm of the product of dynamic modulus and apparent density, according to the model established by Eissa and Kazi (1988), which gave an adjusted value of R^2=0.99

$$\log_{10} E_{\mathrm{st}} = 0.967\ \log_{10}\left(\rho_{\mathrm{bulk}}\ E_{\mathrm{dyn}}\right) - 3.306 \tag{17}$$

Although the coefficient of determination does not vary greatly between both equations, in addition to the higher R-squared value, the non-linear regression fits better to the observed data in that k quickly tends to 1 for modulus values greater than 80 GPa. This expression allows the static

modulus to be calculated from the dynamic modulus in a great variety of rocks. Figure 9 shows a plot of Eqs. (16) and (17), together with the data considered. Although they were not used as part of the regression analysis in this study, the data from the other two authors mentioned previously (Christaras et al. 1994; Jiang and Sun 2011) has also been included.

It should be noted once more that the data used in the regression analysis corresponds to the samples tested in this study (33 samples), plus the data obtained by the authors as part of a previous study (Brotons et al. 2014). This means that the data that was fitted only contained elastic modulus values below 80 GPa. However, when Eq. (17) is extrapolated for higher values, it is coherent with the observations made by Christaras et al. (1994) for samples with a range of moduli of up to 120 GPa. The discontinuous lines in Figure 9 show the extrapolation of Eqs. (16) y (17) beyond the values used for the data fitting.

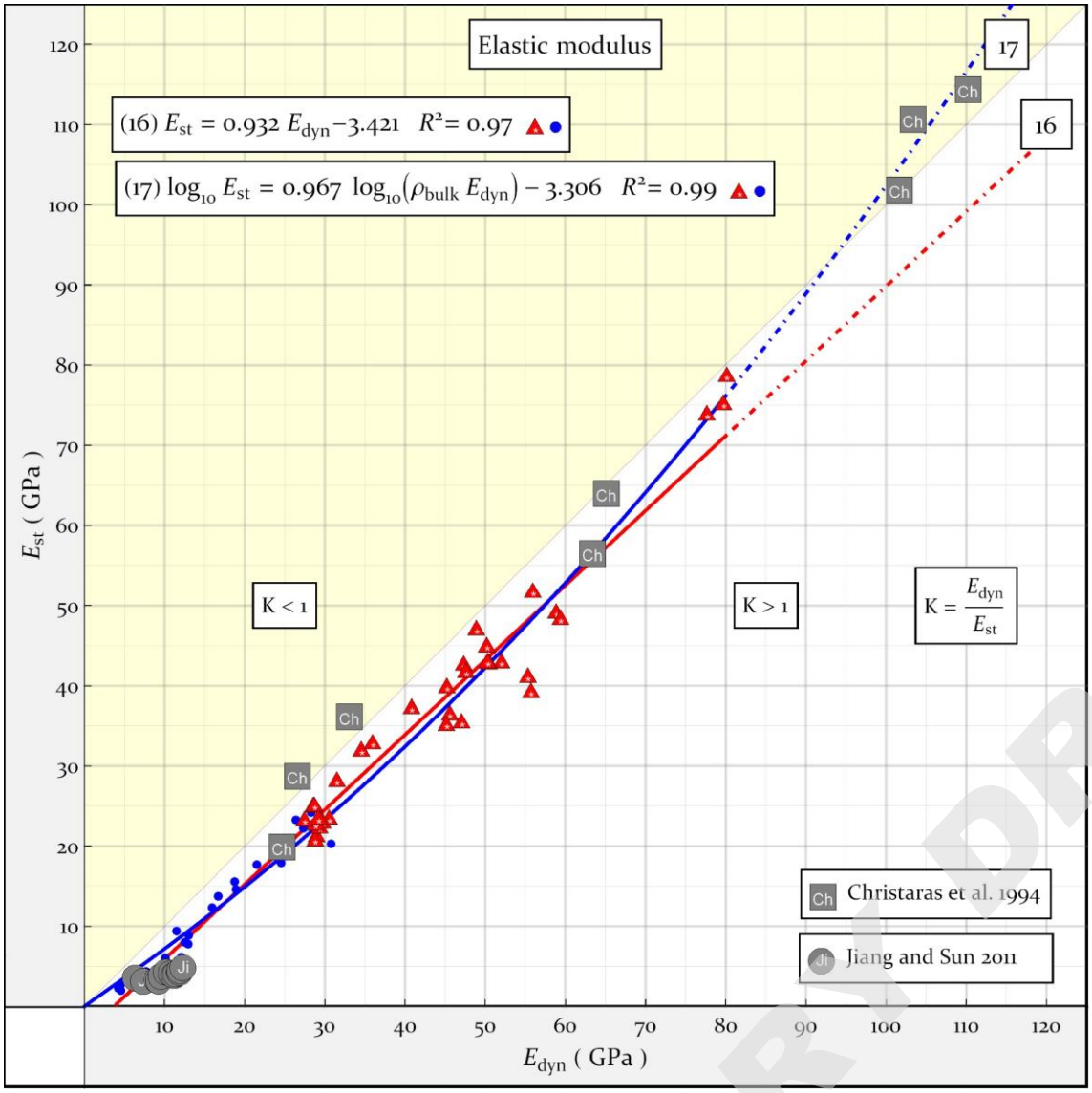

Fig. 9 - *Experimental data and fitting curves obtained by regression (Eqs. 16-17). E_{st}: static modulus. E_{dyn}:dynamic modulus*

It should be noted that the non-linear fitting curve shows that the rate of increase in *k* diminishes as the elastic modulus values decrease in the lower part of the graph (see Figure 9). This trend cannot be conclusively explained by observing the dispersion of data in the range of values below 10-12 GPa. However, the dispersion of *k* values in this type of rocks of very low elastic modulus is inevitable, given that these are generally very porous and heterogeneous, which results in a certain degree of randomness and experimental noise in both static and dynamic measurements. In any case, the trend shown by Eq. (17) is supported by the data obtained for low values above 12 GPa.

At the other extreme, considering compact rocks with a low porosity and high elastic modulus (>80 GPa), the rapid convergence of *k* to 1 can be explained by the fact that the rocks' compactness means they are highly continuous, meaning that their behaviour is similar to the ideal medium (i.e. continuous, elastic and homogenous) for which the equations relating the elastic modulus to ultrasonic wave velocity were derived. In the very low range of moduli (i.e. E_{st}<10 GPa), the reduction in the rate of increase of *k* with the reduction of elastic modulus values can be explained by the characteristics of waves being applied (54-250 kHz). Wave propagation can be drastically altered in deteriorated or very porous materials (hence with a low elastic modulus), which results in their characteristics being reflected more accurately.

For intermediate values (i.e. 20 GPa <E_{st}< 80 GPa), the rocks are not similar to an ideal medium, and so values obtained analytically from ultrasonic wave propagation velocities do not reflect the modulus measured in static tests. In addition, they are not deteriorated sufficiently such that the propagation of waves is greatly affected by the material's porosity. As such, in these conditions the ultrasonic wave propagation velocity does not reflect the mechanical properties of the rock in the same way as static testing.

When considering P wave velocity, a type V equation (see Table 2) was used, giving an equation with a high R-squared value (R^2 =0.99):

$$E_{\mathrm{st}} = 0.679\ {V_{\mathrm{p}}}^{2.664} \tag{18}$$

The advantage of this method lies in the ease of obtaining the V_p parameter, which hence allows the static elastic modulus of rocks to be estimated quickly and reliably. Figure 10 shows the curves corresponding to Eqs. 10-15 and 18 together with the data used in fitting each of the latter two equations. It should be noted that the equation proposed by Najibi et al. (2015) was obtained using test data from 45 limestone core specimens. As such, due to the mineralogy of the samples being the same, the difference in elastic modulus and P wave velocity are exclusively as a result of differences in the distribution and size of pores and fissures.

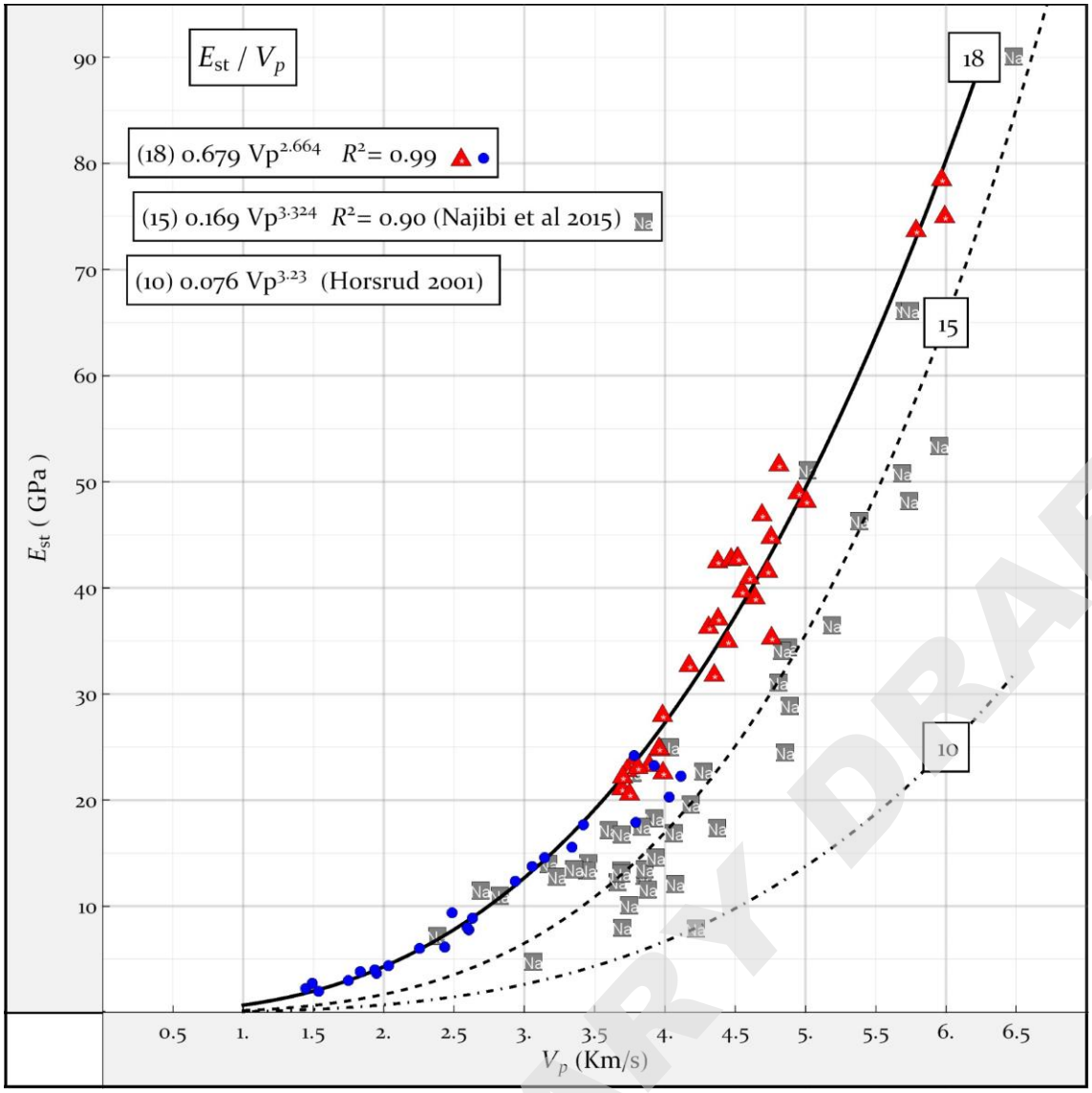

Fig. 10- *Experimental data fitting curve obtained by regression (Eqs. 18) and from a previous study (Eqs. 10-15). E_{st}: static modulus. V_p: P-wave velocity*

The data presented by (Horsrud 2001) was obtained from shale core samples, mainly from the North Sea, which implies that the rocks had a very specific mineralogy characterised by a preponderance of laminar minerals. Additionally, the field cores that were tested were all well preserved such that loss of pore water after coring was prevented, meaning that the rock was tested with its original moisture content. These reasons explain the differences observed in this curve.

5.3. Proposed new models

It should firstly be noted that the type IV equation shown in Table 2 is equivalent to an exponential form.

$$\mathrm{Log}_{10}[E_{\mathrm{st}}] = a\ \mathrm{Log}_{10}\left[\rho E_{\mathrm{dyn}}\right] + b \quad \approx \quad E_{\mathrm{st}} = c\ (\rho E_{\mathrm{dyn}})^{a} \qquad where \qquad c = 10^{b} \tag{19}$$

Using this form, and introducing new parameters and independent variables taken from the rocks in the study, three new models are proposed. These are listed in Table 5, in ascending order of complexity.

Eq.	Relationship	R^2	SSE
(20)	$E_{\mathrm{st}} = 11.531\ {\rho_{\mathrm{bulk}}}^{-0.457} {E_{\mathrm{dyn}}}^{1.251}$	0.993	362.66
(21)	$E_{\mathrm{st}} = 3.97\ 10^{6}\ {\rho_{\mathrm{bulk}}}^{-2.090} {E_{\mathrm{dyn}}}^{1.287}\ n^{-0.116}$	0.994	332.16
(22)	$E_{\mathrm{st}} = 4.71\ 10^{6}\ {\rho_{\mathrm{bulk}}}^{-2.100} {E_{\mathrm{dyn}}}^{1.232}\ n^{-0.129}\ {\sigma_c}^{0.035}$	0.996	190.27

Table 5. *Proposed new correlation models: E_{st}: static modulus (GPa); E_{dyn}: dynamic modulus (GPa); ρ_{bulk}: bulk density (Kg/m^3); n: total porosity (%); σ_c: uniaxial compressive strength (MPa); SSE: sum of squared prediction errors.*

It may be observed that the increasing level of complexity leads to an improved goodness of fit. Figure 11 shows the fitting surface defined by Eq.20, together with the data used for fitting.

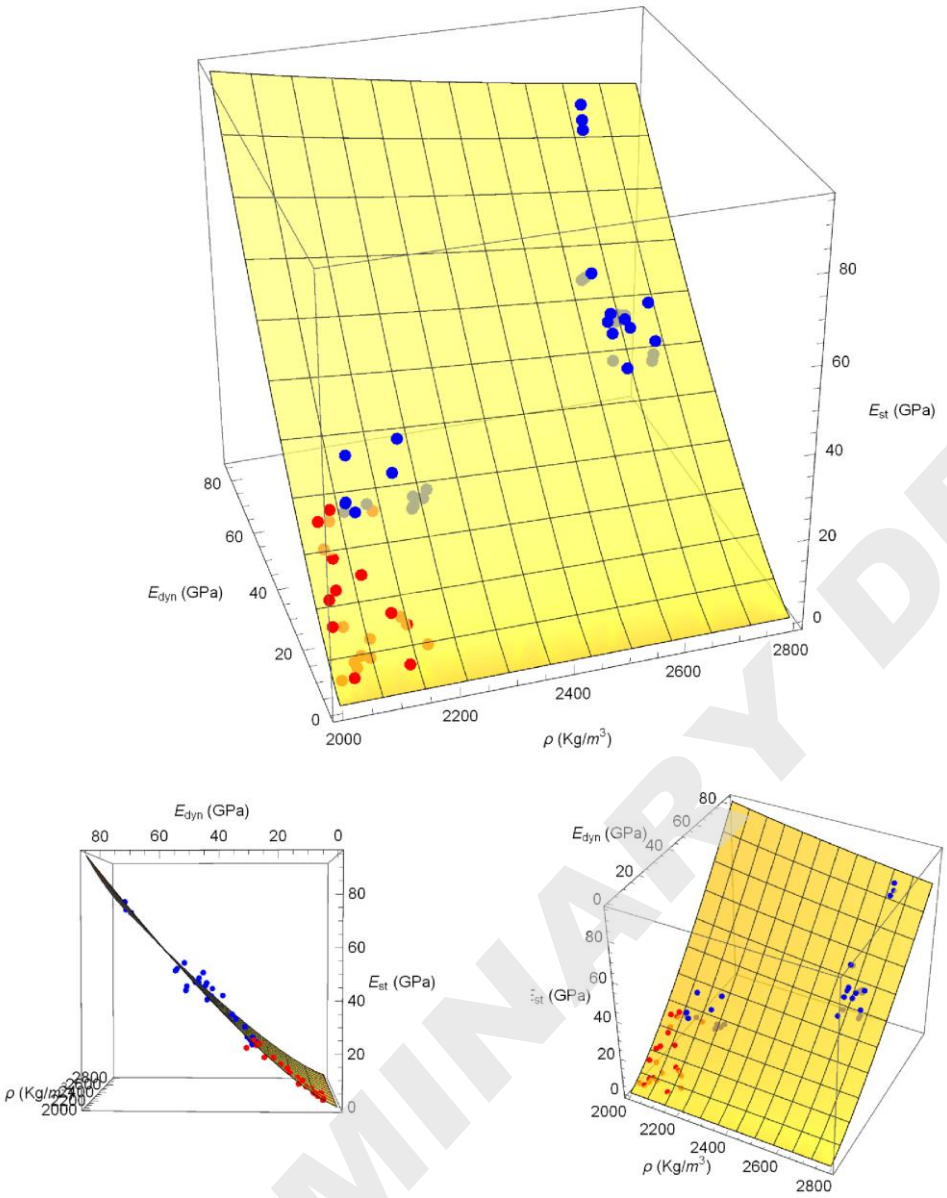

517

518 ***Fig. 11.*** *Experimental data and fitting surface obtained by regression (Eq. 20). E_{st}: static modulus.*

519 *E_{dyn}:dynamic modulus; ρ: bulk density.*

520

521

522

In a real situation where it is necessary to determine the elastic modulus using ultrasound testing, the criteria for choosing between models would depend on the number of variables for which data is available in each case.

1. CONCLUSIONS

In this study, intact rock samples were analysed for their use as structural or ornamental building materials. None of the samples showed macro-fissures or cracks that could have affected static deformability tests or the propagation of ultrasonic waves. The different response of the samples to static and dynamic testing was essentially due to porosity regarding both porous content and type (intercrystalline or interparticle).

In general, high porosity values (>10%) are associated with rocks with low elastic modulus values (<20 GPa) and low apparent density values (<2.2 g/cm^3). In addition, rocks with a high elastic modulus (>80 GPa) show the opposite, i.e. low porosity (<5%) and relatively high apparent density (>2.6g/cm^3). Numerous authors assert that the ratio between elastic moduli ($k=E_{dyn}/E_{sa}$) tends to unity in very stiff and compact rocks, and increases as stiffness and compactness decrease. This is explained by the fact that the presence of voids in the material affects the propagation of ultrasonic waves to a lesser extent than it affects the material's deformability under static loading, meaning that the results obtained from the two techniques diverge. However, it should be noted that the results can be affected by other factors in addition to porosity, as the existence of non-porous materials with *k* values of up to 1.75 demonstrates (Kolesnikov 2009). In rocks, the mineralogical and crystalline nature of the material must also be considered, although it should be noted that fissures and pores do have an important influence.

As such, when seeking to obtain a valid relationship between the static and dynamic elastic modulus, valid for a wide variety of rocks (including a large range of elastic modulus and porosity values, as well as rock characteristics), it is unreasonable to expect a linear relationship dependent on one parameter to give the best results. Consequentially, it becomes necessary to consider another parameter which varies with the stiffness of the rock. Eq. (17) considers the apparent density as an additional variable, indirectly accounting for variations in the porosity and petrographic nature of the rock being considered. This model was proposed by Eissa and Kazi

552 (1988) and was used in a previous study by the authors (Brotons et al. 2014). The previous study
553 considered rocks with an elastic modulus lower than 30 GPa. The small range of elastic moduli
554 considered meant that the non-linear regression model considered gave few advantages over the
555 linear model. In this study, Eq. (17) gave a valid fit for the whole range of moduli considered
556 experimentally (4-80 GPa) and also for data presented by other authors (Christaras et al. 1994)
557 for values up to 120GPa. This allowed the static elastic modulus to be obtained for various
558 different types of rock, using non-destructive testing.

559 Using only one parameter, P-wave velocity, but a non-linear regression model, a goodness of fit
560 similar to Eq. (17) may be obtained with Eq (18). Unfortunately in this case it was not possible to
561 validate this equation for static modulus values greater than 80 GPa.

562 For very high static modulus values (>80 GPa), in which linear models cannot reproduce the
563 convergence of k back towards unity as the elastic modulus increases, Eq. (17) and Eq. (18) do
564 reflect this behaviour.

565 As such, it may be concluded that using the models proposed in this study, the static modulus of
566 elasticity may be reliably derived from the dynamic modulus. This is a great advantage as it allows
567 the process of extracting samples and destructively testing them to be substituted for *in-situ* non-
568 destructive tests. However, it should be noted that the empirical equations presented here, might
569 not work for rocks with more complicated microstructures (cracks, weathering, etc.).

570 It is hence possible, with the aforementioned limitations, to estimate the expected deformability
571 of a material and its actual condition in structures, with a view to assessing the need for
572 maintenance or architectural intervention in buildings or monuments of historical or heritage
573 interest.

574

575 **Acknowledgements**

576 The authors acknowledge the financial support received from the Spanish National project of the
577 Ministry of Economy and Competitiveness by the project BIA2012-34316, and the support of the
578 Generalitat Valenciana by the project ACOMP/2014/289.

579

References

AENOR (2005) UNE-EN 14579. Métodos de ensayo para piedra natural. Determinación de la velocidad de propagación del sonido. Asociación Española de Normalización y Certificación

AENOR (2007) UNE-EN 1936: Métodos de ensayo para piedra natural. Determinación de la densidad real y aparente y de la porosidad abierta y total vol 1. Asociación Española de Normalización y Certificación, Spain

Al-Shayea NA (2004) Effects of testing methods and conditions on the elastic properties of limestone rock Engineering Geology 74:139-156 doi:10.1016/j.enggeo.2004.03.007

Ameen MS, Smart BG, Somerville JM, Hammilton S, Naji NA (2009) Predicting rock mechanical properties of carbonates from wireline logs (A case study: Arab-D reservoir, Ghawar field, Saudi Arabia) Marine and Petroleum Geology 26:430-444

Assefa S, McCann C, Sothcott J (2003) Velocities of compressional and shear waves in limestones Geophysical prospecting 51:1-13

Benavente D, García del Cura MA, Bernabéu A, Fort A, La Iglesia A, Ordóñez S (2005) Use of the microcrystalline limestone as building material: the "Gris Pulpis" case Materiales de Construcción 55:5-23

Benson P, Meredith P, Platzman E, White R (2005) Pore fabric shape anisotropy in porous sandstones and its relation to elastic wave velocity and permeability anisotropy under hydrostatic pressure International Journal of Rock Mechanics and Mining Sciences 42:890-899

Brotons V, Ivorra S, Martínez-Martínez J, Tomás R, Benavente D (2013) Study of creep behavior of a calcarenite: San Julián´s stone (Alicante) Materiales de Construcción 63:581-595 doi:10.3989/mc.2013.06412

Brotons V, Tomás R, Ivorra S, Grediaga A (2014) Relationship between static and dynamic elastic modulus of a calcarenite heated at different temperatures: the San Julián's stone Bulletin of Engineering Geology and the Environment 73:791-799 doi:DOI 10.1007/s10064-014-0583-y

Ciccotti M, Mulargia E (2004) Differences between static and dynamic elastic moduli of a typical seismogenic rock Geophysical Journal International 157:474-477 doi:10.1111/j.1365-246X.2004.02213.x

Christaras B, Auger F, Mosse E (1994) Determination of the moduli of elasticity of rocks. Comparison of the ultrasonic velocity and mechanical resonance frequency methods with direct static methods Materials and Structures 27:222-228 doi:10.1007/bf02473036

Dunham RJ (1962) Classification of Carbonate Rocks According to Depositional Texture. In: Ham WE (ed) Classification of Carbonate Rocks. American Association of Petroleum Geologists, pp 108-121

Eissa EA, Kazi A (1988) Relation between static and dynamic Young´s Moduli of rocks Int J Rock Mech Min Sci 25:479-482 doi:10.1016/0148-9062(88)90987-4

García-del-Cura M, Benavente D, Martínez-Martínez J, Cueto N (2012) Sedimentary structures and physical properties of travertine and carbonate tufa building stone Construction and Building Materials 28:456-467

627 Guéguen Y, Palciauskas V (1994) Introduction to the physics of rocks. In: Press PU (ed).
628 Princeton, New Jersey (EE.UU), p 294 pp
629 Heap MJ, Faulkner DR (2008) Quantifying the evolution of static elastic properties as crystalline
630 rock approaches failure International Journal of Rock Mechanics and Mining Sciences
631 45:564-573 doi:http://dx.doi.org/10.1016/j.ijrmms.2007.07.018
632 Horsrud P (2001) Estimating Mechanical Properties of Shale From Empirical Correlations
633 Society of Petroleum Engineers, SPE doi:10.2118/56017-pa
634 Ide JM (1936) Comparison of statically and dynamically determined young's modulus of rocks
635 Proceedings of the National Academy of Sciences of the United States of America
636 22:81-92 doi:10.1073/pnas.22.2.81
637 ISRM (1979) Suggested Method for Determining the Uniaxial Compressive Strength and
638 Deformability of Rock Materials ISRM Suggested Methods 2:137-140
639 Jiang J, Sun J-z (2011) Comparative study of static and dynamic parameters of rock for the
640 Xishan Rock Cliff Statue Journal of Zhejiang University SCIENCE A 12:771-781
641 doi:10.1631/jzus.A1100003
642 King MS (1983) Static and dynamic elastic properties of rocks from the canadian shield
643 International Journal of Rock Mechanics and Mining Sciences 20:237-241
644 doi:10.1016/0148-9062(83)90004-9
645 Kolesnikov YI (2009) Dispersion effect of velocities on the evaluation of material elasticity J Min
646 Sci 45:347-354
647 Lacy L (1997) Dynamic Rock Mechanics Testing for Optimized Fracture Designs. Paper SPE
648 38716 presented at the SPE Annual Technical Conference and Exhibition, San Antonio,
649 Texas, USA, 5–8 October.
650 Martinez-Martinez J, Benavente D, Garcia-del-Cura MA (2011) Spatial attenuation: The most
651 sensitive ultrasonic parameter for detecting petrographic features and decay
652 processes in carbonate rocks Engineering Geology 119:84-95
653 doi:10.1016/j.enggeo.2011.02.002
654 Martinez-Martinez J, Benavente D, Garcia-del-Cura MA (2012) Comparison of the static and
655 dynamic elastic modulus in carbonate rocks Bulletin of Engineering Geology and the
656 Environment 71:263-268 doi:10.1007/s10064-011-0399-y
657 Najibi AR, Ghafoori M, Lashkaripour GR (2015) Empirical relations between strength and static
658 and dynamic elastic properties of Asmari and Sarvak limestones, two main oil
659 reservoirs in Iran Journal of Petroleum Science and Engineering 126
660 Nur A, Wang Z (1999) Seismic and Acoustic Velocities in Reservoir Rocks: Recent Developments
661 Society of Exploration Geophysicists 10
662 Palchik V, Hatzor Y (2002) Crack damage stress as a composite function of porosity and elastic
663 matrix stiffness in dolomites and limestones Engineering Geology 63:233-245
664 Vanheerden WL (1987) General relations between static and dynamic moduli of rocks Int J
665 Rock Mech Min Sci 24:381-385
666 Vergara L et al. (2001) NDE ultrasonic methods to characterise the porosity of mortar NDT & E
667 International 34:557-562

668

669